






Article

Enhancement of Solar PV Hosting Capacity in a Remote Industrial Microgrid: A Methodical Techno-Economic Approach

Shaila Arif ¹, Ata E Rabbi ^{1,*}, Shams Uddin Ahmed ², Molla Shahadat Hossain Lipu ³, Taskin Jamal ¹, Tareq Aziz ¹, Mahidur R. Sarker ⁴, Amna Riaz ⁵, Talal Alharbi ^{6,*} and Muhammad Majid Hussain ⁷

- ¹ Department of Electrical and Electronic Engineering, Ahsanullah University of Science and Technology, Dhaka 1208, Bangladesh; shaila.arif.eee@aust.edu (S.A.); t.jamal.eee@aust.edu (T.J.); taziz.eee@aust.edu (T.A.)
² Energrid Engineers Ltd., Dhaka 1212, Bangladesh; shams.shobuz@gmail.com
³ Department of Electrical and Electronic Engineering, Green University of Bangladesh, Dhaka 1207, Bangladesh; shahadat@eee.green.edu.bd
⁴ Institute of IR 4.0, Universiti Kebangsaan Malaysia, Bangi 43600, Malaysia; mahidursarker@ukm.edu.my
⁵ Department of Electrical Engineering, Bahauddin Zakariya University, Multan 60000, Pakistan; amna.riaz@bzu.edu.pk
⁶ Department of Electrical Engineering, College of Engineering, Qassim University, P.O Box 6677, Buraydah 51452, Qassim, Saudi Arabia
⁷ Department of Electrical and Electronic Engineering, University of South Wales, Pontypirdd CF37 1DL, UK; muhammad.hussain@southwales.ac.uk
* Correspondence: ata_e_rabbi.eee@aust.edu (A.E.R.); atalal@qu.edu.sa (T.A.)



check for updates

Citation: Arif, S.; Rabbi, A.E.; Ahmed, S.U.; Hossain Lipu, M.S.; Jamal, T.; Aziz, T.; Sarker, M.R.; Riaz, A.; Alharbi, T.; Hussain, M.M. Enhancement of Solar PV Hosting Capacity in a Remote Industrial Microgrid: A Methodical Techno-Economic Approach. *Sustainability* **2022**, *14*, 8921. <https://doi.org/10.3390/su14148921>

Academic Editors: Mouloud Denai, Mustapha Hatti, Azeddine Draou and Pedram Asef

Received: 23 May 2022

Accepted: 1 July 2022

Published: 21 July 2022

Publisher's Note: MDPI stays neutral with regard to jurisdictional claims in published maps and institutional affiliations.



Copyright: © 2022 by the authors. Licensee MDPI, Basel, Switzerland. This article is an open access article distributed under the terms and conditions of the Creative Commons Attribution (CC BY) license (<https://creativecommons.org/licenses/by/4.0/>).

Abstract: To meet the zero-carbon electricity generation target as part of the sustainable development goals (SDG7), remote industrial microgrids worldwide are considering the uptake of more and more renewable energy resources, especially solar PV systems. Estimating the grid PV hosting capacity plays an essential role in designing and planning such microgrids. PV hosting capacity assessment determines the maximum PV capacity suitable for the grid and the appropriate electrical location for PV placement. This research reveals that conventional static criteria to assess the PV hosting capacity fail to ensure the grid's operational robustness. It hence demands a reduction in the theoretical hosting capacity estimation to ensure grid compatible post-fault voltage and frequency recovery. Energy storage technologies, particularly fast-responsive batteries, can potentially prevent such undesirable scenarios; nevertheless, careful integration is required to ensure an affordable cost of energy. This study proposes a novel methodical techno-economic approach for an off-grid remote industrial microgrid to enhance the PV hosting capacity by integrating battery energy storage considering grid disturbance and recovery scenarios. The method has been validated in an industrial microgrid with a 2.6 MW peak demand in a ready-made garment (RMG) factory having a distinctive demand pattern and unique constraints in remote Bangladesh. According to the analysis, integrating 2.5 MW of PV capacity and a 1.2 MVA battery bank to offset existing diesel and grid consumption would result in an energy cost of BDT 14.60 per kWh (USD 0.1719 per kWh). For high PV penetration scenarios, the application of this method offers higher system robustness, and the financial analysis indicates that the industries would not only benefit from positive environmental impact but also make an economic profit.

Keywords: PV hosting capacity; industrial microgrid; RMG; PV penetration; PV-battery system

1. Introduction

Rapid industrialization has resulted in a dramatic increase in product demand for various sectors throughout the world. In every country, large and medium-sized industries are expanding at a faster rate than ever before. These space-consuming industries locate their technology, machinery, and office spaces mostly in remote regional locations based on the availability of land-area, energy resources, workforce, transportation, and logistics. It

may be mentioned that a large number of these distant regions are off-grid, and extension of the central electric grid to those regions is not conceivable owing to techno-economic issues in developing countries. As a result, there is always a concern about ensuring a dependable and high-quality power supply to build sustainable growth. This influences respective countries' ability to achieve their sustainable development goals by 2030.

Being one of the developing countries, Bangladesh is also reaping the benefits of fast industrialization. Due to the rapid expansion of related industries, the once agro-based economy has shifted to an industrial economy. The ready-made garments (RMG) business plays a considerable role in its economy among all other local industries. In 2021, Bangladesh's textile sector was the world's second-largest exporter, hosting more than 4000 RMG factories [1]. Bangladesh has the highest number of LEED (Leadership in Energy and Environmental Design) platinum-rated garment factories globally, owing to industry owners' emphasis on a dependable and sustainable power supply system for their businesses [2]. According to the PV magazine, more than 500 enterprises have recently registered to make their production facilities more environment friendly by utilizing the net-metering facility offered by the utility [3]. According to some government bodies, these factories consume almost one-sixth of the country's energy consumption, and through the low-cost financing mechanism, the adoption of net-metered solar PV systems would significantly offer better energy efficiency and industry performance.

In the maximum of these RMG industries, the manufacturers opt to control their power supply on their own in addition to the grid supply. Many of these RMG manufacturers are located in remote or off-grid/isolated areas where grid electricity is either of poor quality or non-existent. Traditionally, diesel-powered systems have primarily been prioritized to the electrification of the industry as a result of their dispatchable nature, along with trouble-free installation features and lower initial costs [4]. However, fluctuating prices, the fuel supply uncertainty and the dependent supply chain mechanisms tend to obstruct the availability of fuel and fuel trade. As an alternative, solar PV and wind energy systems offer significantly less environmental impact than diesel-based energy systems and offer an affordable and reliable energy supply. However, considering the local context, the only available source is the solar PV in this case. This has opened the door to incorporating locally exploitable clean energy resources into the generation mix. Integrating these systems can help save money by reducing the dependency on the grid and taking advantage of government rebates and facilities. The regular operation and maintenance costs and the initial investment of the solar PV systems have been decreasing in recent years. Hence, in many regions, solar PV incorporated hybrid energy systems provide a cost-effective and technically reliable solution to the demand; global studies conducted by Jamal et al., and El-houari et al., suggest this finding [4–6]. To incorporate such hybrid energy system, a microgrid is a well-accepted concept in remote regions and is becoming more popular day by day [7,8].

The entire capacity of the PV systems that may be integrated into a particular microgrid without exceeding steady-state operating constraints is referred to as the hosting capacity (HC) of PV. The HC of the PV system in a network gives an indication of the theoretical maximum level of total PV system capacity that is allowed in the network. The HC estimation needs to consider the network demand profile, generator dispatch profile, operating reserve, PV system's diversity and fluctuation factors, step load capacities of generators, and generator startup and minimum run time etc. [9]. Hence, the majority of HC evaluations presented in the literature are based on steady-state analyses. HC can alter depending on the reference parameter, network conditions, topology, location, and PV deployment scenario. HC is, therefore, not a unique value, and it greatly depends on the appropriate selection of the mentioned performance indices and their limits [10]. According to [11], some of the notable challenges for remote PV-diesel electricity networks include maintaining supply quality, legacy infrastructure, spinning (i.e., operating) reserve policy, etc. With an increased share of PV, various switching operations play influential roles in the network [12]. Studies in [13] show that operation may become unstable with diesel

generators turned off in a diesel-PV based microgrid. Ismael et al. also stated that HC should be calculated regularly based on various performance indices such as voltage and frequency variations, power quality, etc. [10]. In references [14–25], the energy systems are designed and analyzed through various techno-economic studies. Calculating the HC gives the assessment of PV capacity to be integrated into the grid without violating the grid code. A few studies, including [26–28] identified the necessity of considering critical technical scenarios along with the investigation of the economic feasibility of industry operations. However, to the best of the authors' knowledge, the existing literature did not carry out detailed studies taking the issues of varying operation scenarios under system disturbances. The comparison between this work and other similar works is given in Table 1.

Table 1. Comparison between this work with other similar studies.

Reference No	Grid Connectivity	Energy System	HC Analysis	System Robustness Check	Optimization
[14]	Off-grid	Diesel, PV + Diesel, PV + Diesel + Battery, Wind + Diesel, Wind + Diesel + Battery, Diesel + Battery, PV + Wind + Diesel, PV + Wind + Diesel + Battery	No	No	Yes
[15]	Off-grid	PV + Diesel + Battery, PV + Wind + Diesel + Battery, PV + Battery, Wind + Diesel + Battery, Diesel	No	No	Yes
[16]	Off-grid	PV, PV + Battery	No	No	No
[17]	Off-grid	PV	No	No	No
[18]	Off-grid	PV, Wind, PV + Wind	No	No	Yes
[19]	Off-grid	PV	No	No	Yes
[20]	On-grid and off-grid	Grid + PV, PV + Battery	No	No	Yes
[21]	On-grid and off-grid	Grid + PV, Grid + PV + Battery, PV + Battery	No	No	Yes
[22]	On-grid	PV	No	No	Yes
[23]	On-grid	Grid + PV + Wind + Battery	Yes	No	Yes
[24]	On-grid	Grid + PV	Yes	No	No
[25]	On-grid	Grid + PV, Grid + Wind, Grid + PV + Wind	No	No	Yes
This paper	Off-grid	Diesel + PV + Battery	Yes	Yes	Yes

This study showcases that HC determination using only static parameters is merely a theoretical capacity, and this capacity has to be sacrificed under extreme operation scenarios. A step by step methodology is thus proposed whereas battery energy storage system (BESS) is integrated to stabilize the system dynamics and enhance the PV HC of the system. Adopting this strategy evades the risk of sacrificing potential PV capacity. An economic feasibility study followed by a literature evaluation with earlier studies shows the eminence of the proposed method. The cautionary planning approach proposed in this work is expected to be helpful in the future development of PV integrated industries operating in the off-grid mode in remote areas. The proposed methodology is globally applicable; however, the simulation and the method's efficacy have been validated using an RMG factory grid information from Bangladesh. Due to network information intellectual property issues, data scaling has been employed wherever necessary.

The core novelty and contribution offered in this study can be summarized as follows:

- Developing a methodological approach for evaluating the PV hosting capacity for an industrial microgrid considering operational issues
- Validating the method by assessing the robustness against significant disturbances in an industrial microgrid
- Evaluating the techno-economic feasibility of high penetration of PV scenarios for a test case scenario (industrial microgrid)
- Demonstrating a systematic pathway to introduce sustainable energy technologies for ready-made garment industries to address the requirements for a green factory, which would, in the long run, attract more buyers and investors
- To the best of the authors' knowledge, this methodological approach is one of its kind, found in the literature regarding the hybridization of the unique electrical power system network of the ready-made garment industry in a developing country like Bangladesh

The article is organized as follows: Section 2 discusses the concept of HC of PV systems in the grid and presents the issues of an industrial microgrid that need particular attention

while determining the HC. Section 2 also presents the step-wise methodology to determine the ultimate HC of a microgrid. Results and discussions are presented in Section 3, and Section 4 draws conclusions highlighting the findings.

2. Materials and Methods

2.1. Solar PV Hosting: Performance Indices and Challenges in Remote Industrial Microgrids

Uncertainties in solar PV generation impose challenges on the control of a microgrid (MG). Due to the intermittent nature of solar PV and wind, different issues such as voltage flicker and voltage fluctuations occur in an MG. Poor connectivity with the grid in a remote power system raises several technical issues, including voltage drops, low power quality, and high line losses. These issues make the MG less economically feasible in remote areas for grid-connected operations [29]. Due to different characteristics and types of loads and PV uncertainties, a remote MG's key challenges are maintaining the voltage and frequency within a permissible range. The PV HC of a network gives an indication of the allowed level of total PV systems' capacity in the network. The technical issues that are considered by PV HC calculation are based on the static and dynamic system performance [12].

The key components of the industrial microgrid considered in this work are portrayed in Figure 1. BESS has been used increasingly along with solar PV in an MG due to its ability to facilitate the MG to operate in the off-grid mode by providing synthetic inertia. In addition to that, BESS is also helpful in a power system to smooth the supply and demand differences, which is hampered by the intermittent nature of solar PV or fluctuation of loads [30]. The application of BESS has also demonstrated superior system performance in terms of restoring a system during post fault scenarios. Thus, BESS has become a proven technology to enhance system resiliency. However, regarding the integration and operation of BESS in microgrids, consideration of economic factors play a critical role in determining the system configuration and levelized cost of energy (LCOE) [31]. Hence, economic analysis of the whole procedure is recommended to investigate the techno-economic feasibility of a microgrid consisting of PV-BESS systems [32].

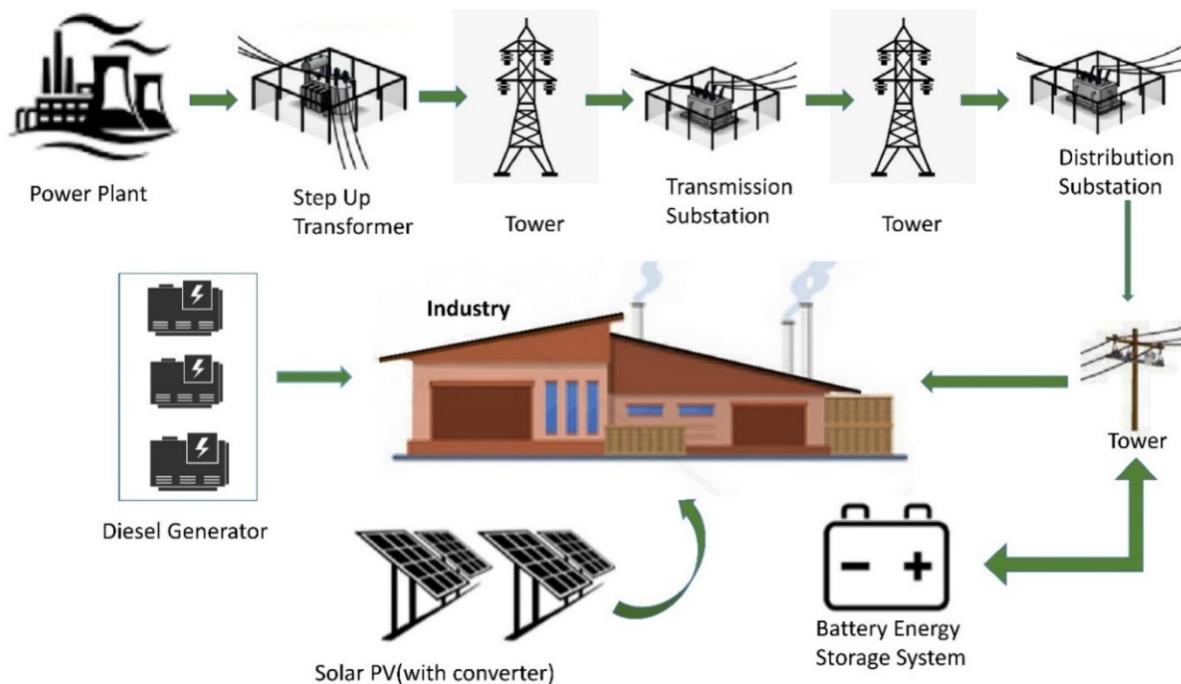


Figure 1. Schematic diagram of the major components of the industrial system.

As mentioned earlier, the HC of PV system for a specific power system can be defined as the amount of PV generation capacity (usually for distributed generation) integrated into the power system, above which the system's operating conditions are violated [10,33–35].

The HC of PV in a network can be determined by an iterative method considering the system power factor, voltage regulation and equipment loading [33]. HC of the respective network also depends on the characteristics of the network, load and generation stream [36]. Remote networks have lower estimated HC values than urban networks due to the topological and electrical characteristics of the weak network and voltage rise difficulties at the end of lengthy feeders [37]. An extensive literature review reveals a few standard criteria for determining the HC, based on analyzing the overvoltage, thermal overloading, electrical power loss, power quality and protection problems [10]. Some of these static performance issues are briefly described as follows:

(1) *Voltage limits violations*

The major voltage issues due to a high PV penetration include overvoltage at the end of the feeder, flicker, voltage sag and swell. Among these, overvoltage is the dominant issue. Fatima et al. have discussed five commonly used voltage standards such as the European standard ($\pm 10\%$ of nominal voltage, V_N), German standard ($+3\%$ of V_N), American standard ($\pm 5\%$ of V_N), Australian standard ($-6\%/+10\%$ of V_N) and Canadian standard ($\pm 6\%$ of V_N) [37]. Increasing PV penetration without proper technical estimation violates the overvoltage range in the respective network, and thus, an upper limit on the aggregated PV capacity is required. Another issue is flickering, which originates due to the excessive amount of renewables in the system and propagates to the distribution feeder [38]. The variability characteristics of PV output and lack of system inertia due to high PV penetration in an MG leads to frequent flickering, voltage sag and swell problems [39].

(2) *Capacity and thermal limits*

The current capacity of cables and transformers impose a limit in integrating a higher amount of PV. Several countries and regions have different overload limits to incorporate PVs in an industrial MG. Fatima et al. have discussed several overload limits for transformers and cables, including 85%, 100%, 150% and 187.5% of nominal values across different countries [37].

(3) *Unbalance*

The negative sequence unbalance is another challenge while integrating more PV generation in an MG. The limit of this unbalance is being set to 2% by IES standards [37], and [37] have addressed different negative sequence unbalance limits such as 1%, 1.3%, 2% and 3% of V_N [37].

(4) *Harmonics*

The authors in [40] investigated a rural low voltage residential distribution network for maximal PV penetration using harmonics as a limiting factor. The operation of a renewable integrated MG is adversely affected by harmonics generated by power electronics converter interfaced with solar PV. Harmonics are also generated due to the non-linearity of loads in an MG. The operators must limit these harmonics by limiting the third harmonic distortion (THD) to ensure power quality. Several studies have taken maximum THD as 6.1% and 5%. Harmonics reduces energy transfer capability as well as increases system loss [37].

The indices discussed above primarily play a significant role in determining solar PV hosting capacity in a large network as well as in microgrids strongly connected to a grid. In large power systems, a large number of conventional generators take part in primary control with sufficient droop characteristics. This strategy mitigates any sudden imbalance between load and generation and keeps the frequency within the permissible range. When an MG is strongly connected to the grid, it gets high inertia support to mitigate any frequency issue caused by sudden disturbances such as faults, large load or generation change. However, the inertia support is insufficient in off-grid operation due to small-sized conventional generators, and the high shares of power electronic converter interfaced PVs. As a result, sudden frequency issues due to any disturbance are hard to mitigate. This eventually causes cascading failure and tripping of DGs according to various interconnection policies in practice across utilities [41].

In the off-grid operation of industrial MG, motor starting events may lead to generator swing [42]. Reference [43] have analyzed the effect of motor starting in a weak grid having a mix of conventional and inverter-based generation. The large currents caused by the starting motors may easily exceed the current limit of inverter-based generation. Large disturbance scenarios, i.e., faults or loss of generation or significant load increment, may cause a severe impact on MG operations [44]. Hence, wide integration of solar PV (unlimited HC) might not always ensure grid-compatible operation, especially under post-fault conditions. The next section presents a methodological development of a unique approach that showcases the limitations of theoretical HC under post-fault scenarios and proposes the enhancement of HC of PV system with integration of BESS.

2.2. Proposed Methodology Considering Techno-Economic Issues

The proposed methodology finds out technically feasible HC of solar PV in an industrial microgrid through two principal steps.

Step 1: Evaluate HC of test system considering static operational issues and find its robustness against significant disturbances

Step 2: Overcoming technical obstacles to reach target HC

These two steps are followed by a feasibility study to assess the economic validity of the newly determined HC. A necessary flowchart to understand the methodology is shown in Figure 2. The steps can be described as follows:

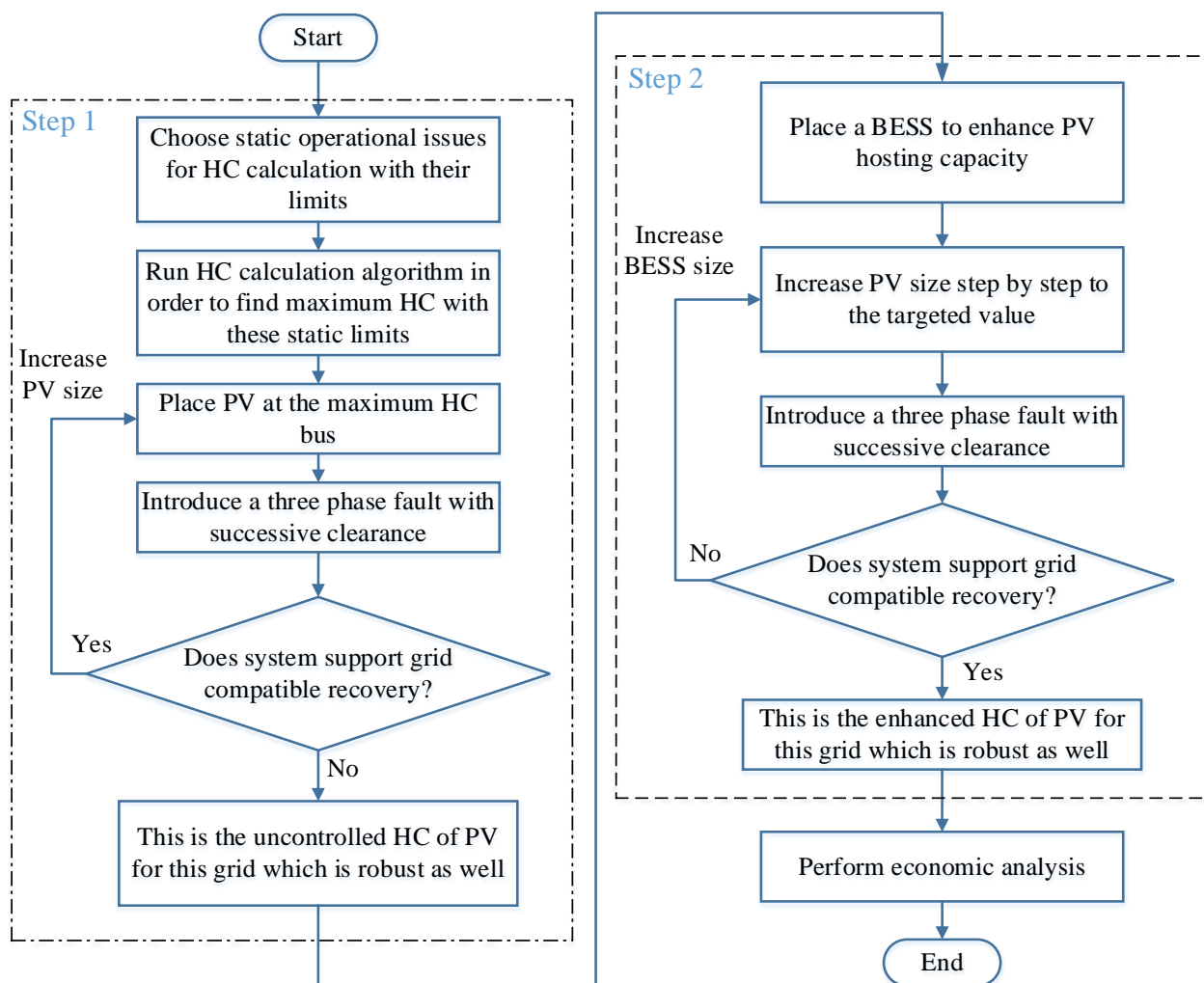


Figure 2. Flowchart of the methodology to incorporate maximum PV in an industrial MG with fault tolerance.

2.2.1. Step 1: Evaluate HC of Test System Considering Static Operational Issues and Find Its Robustness against Significant Disturbances

There are various ways to determine the HC of the PV system in a network mentioned earlier in Section 2.1. There are different criteria, on which the HC calculation is based, such as voltage and frequency variations, overvoltage, thermal overloading, electrical power loss, power quality and protection problems. The first step of this methodology is to find out the HC of PV of this industrial MG considering some static criteria and then find the system's robustness against a significant disturbance in the presence of PV. Calculation of PV HC is an iterative method that is based on the binomial search method [45]. The algorithm continues until convergence is obtained without violations within the maximum number of iterations. This value can be said to be the maximum HC for that bus in the system. After getting the maximum HC value for one bus, the maximum HC for the rest of the buses in the system is obtained by the same algorithm. The bus with maximum PV HC will be sorted after completing the above process. With this analysis, it will be easier to decide the location and the maximum allowable size of PV that does not violate the considered criteria. To calculate the PV HC, the formulations are given below:

$$\text{Objective function : Maximize, } P_{PVi} \quad (1)$$

$$\text{Subject to, } P_i = \sum_{k=1}^n |V_i||V_k|(G_{ik}\cos\theta_{ik} + B_{ik}\sin\theta_{ik}) \quad (2)$$

$$\text{Constraints : } V_{min} \leq V_i \leq V_{max} \quad (3)$$

$$I_{ik} \leq I_{ikmax} \quad (4)$$

where,

P_{PVi} = Active power injection by solar PV at bus i

P_i = Total active power of bus i

G_{ik} = line conductance between bus i and bus k .

B_{ik} = line susceptance between bus i and bus k .

V_{min} = Lower voltage magnitude boundary of bus i

V_i = Voltage magnitude of bus i

V_{max} = Upper voltage magnitude boundary of bus i

I_{ik} = Line current between bus i and bus k

I_{ikmax} = Maximum allowable line current between bus i and bus k (thermal constraint)

Now to observe whether this sizing is technically robust or not, a system disturbance is introduced. In this study, a 3-phase short circuit fault is placed at the bus having the maximum load with successive clearance after 0.2 s. If the system can withstand the fault, i.e., the post fault voltage and current are within the allowable limit set by IEEE std. 1547-2018 [46], it only can be said that the system is technically robust; otherwise, not. Details of the regulations stated in IEEE std. 1547-2018 have been listed in the section: Grid Rules. If the system fails to maintain post fault voltage and frequency within the permissible range, the size of PV is reduced gradually until the system is capable of maintaining allowable post fault voltage and frequency. This reduced size of PV is called the uncontrolled HC (achieved HC without the support of BESS) for this system.

2.2.2. Step 2: Overcoming Technical Obstacles to Reach Target HC

To further increase the share of PV in the system, a BESS is introduced. Now, the system goes through a resiliency test. If the post fault voltage and frequency stay within the permissible limit (according to IEEE std. 1547-2018), more PV generation is injected until the system fails to stay within the allowable post fault voltage and frequency barrier when the fault condition is simulated in the system during the resiliency test. Then the size of BESS is increased to incorporate more PV in the system until the PV size reaches the maximum (with the support of BESS).

Grid Rules:

The interconnection policy plays an important role in MG operation and control. According to IEEE std. 1547-2018, any distributed generation (DG), or PV systems in this study are subjected to mandatory tripping in case of any voltage and frequency deviation from its nominal values after a specific ride through time [46]. The mandatory trip setting due to voltage and frequency violations are given in Table 2. The ranges of allowable settings given in the tables do not require the DG to ride through this magnitude and duration of voltage and frequency. The local DG operators can set the voltage and frequency threshold with a specific clearing time for DG tripping due to abnormal voltage and frequency within the specified limits. It can be seen that the continuous operational voltage range is $0.88 \text{ p.u.} \leq V \leq 1.10 \text{ p.u.}$ and the continuous operational frequency range is $0.975 \text{ p.u.} \leq f \leq 1.02 \text{ p.u.}$

Table 2. DER Response (shall trip) to Abnormal Voltages and Frequencies.

Shall Trip Function	Default Setting		Range of Allowable Settings	
	Voltage (p.u. of Nominal Voltage)	Clearing Time (s)	Voltage (p.u. of Nominal Voltage)	Clearing Time (s)
Over voltage, OV2	1.20	0.16	fixed at 1.20	fixed at 0.16
Over voltage, OV1	1.10	2.0	1.10–1.20	1.0–13.0
Under voltage, UV1	0.70	2.0	0.0–0.88	2.0–21.0
Under voltage, UV2	0.45	0.16	0.0–0.50	0.16–2.0
	Frequency (p.u)	Clearing time (s)	Frequency (p.u)	Clearing time (s)
Over frequency, OF2	1.033	0.16	1.03–1.1	0.16–1000.0
Over frequency, OF1	1.02	300.0	1.017–1.1	180.0–1000.0
Under frequency, UF1	0.975	300.0	0.833–0.983	180.0–1000
Under frequency, UF2	0.942	0.16	0.833–0.95	0.16–1000

2.3. Evaluating Economic Feasibility of Proposed HC

Following the completion of the technical study, the techno-economic analysis is performed to assess the economic feasibility of the technical solution proposed in the flowchart of Figure 2. The techno-economic analysis takes into account the initial investment of the system, generators, PV and BESS plants; their operational and maintenance cost; fuel supply cost, etc. Among all feasible technical solutions obtained in steps 1 and 2, the one with the lowest levelized cost of energy (LCOE) may be designated as the PV's techno economically viable HC.

The first part of the analysis optimizes the size of system components, such as PV systems, batteries and inverters. As PV-battery systems are integrated into the reference case, the system economic dispatch can be formulated as:

$$\text{Objective Functions: Minimize [OMC (} P_{gi}, PV_i, \text{ BESS, OR)]} \quad (5)$$

$$\text{Minimize [F(} P_{gi}\text{)]} \quad (6)$$

$$\text{Minimize [Excess Electricity] and} \quad (7)$$

$$\text{Maximize } \sum_i^N PV_i \quad (8)$$

Subject to constraints:

$$L(t) = OR(t) + P(t) \quad (9)$$

$$\sum_i^M P_{gi} + \sum_i^N PV_i + \sum BESS \geq L(t) \quad (10)$$

$$\alpha L(t) + \beta PV_i = OR(t) \quad (11)$$

$$P_{gi}^{min} \leq P_{gi} \leq P_{gi}^{rated} \quad (12)$$

$$P_{gi}^{min}(t) \geq \gamma P_{gi}^{rated} \quad (13)$$

$$SOC^{min} \leq SOC(t) \leq SOC^{max} \quad (14)$$

$$t_{gi}^{min} \geq 30 \text{ min} \quad (15)$$

where,

OMC = combined operation and maintenance costs of conventional generators, PV systems, battery bank and operating reserve;

F = fuel usage;

P_{gi} = power generation from the i -th conventional generator;

PV_i = power generation from the i -th PV system;

OR = operating reserve;

$P(t)$ = power generation capacity at any time ' t ';

$L(t)$ = load plus losses at any time ' t ';

α = percentage of the load at any time ' t ';

β = percentage of PV output at any time ' t ';

M = total number of conventional generators;

N = total number of PV systems;

γ = minimum loading of the i -th conventional generator;

SOC = battery bank state of charge;

t_{gi}^{min} = minimum runtime (minute) of the i -th conventional generator.

The “load following” controller has been deployed to address the economic dispatch problem [47]. The least cost-optimal combination in both techniques allows dispatchable sources to generate and fulfil load demand and reserve needs. The fixed and marginal costs of dispatchable sources were considered while determining the cost.

3. Results

3.1. Test System

An RMG factory located in Gazipur, Bangladesh, has been chosen to validate the methodology. The factory is a modern one having all the necessary machines for producing RMG products for exports. Based on the collected feeder information and load consumption data, the daily load profile is plotted in Figure 3 and is used for techno-economic analysis. The daily peak load is 2656.46 kW, and the minimum load is 1402.52 kW. The factory runs in three shifts per day that starts at 8.00 a.m. and ends at 8.00 p.m. Most machines such as sewing machines, manual linking machines and iron tables run in between these hours. From 1.00 p.m. to 2.00 p.m., the factory workers get a lunch break. The knitting machines run 24 h a day continuously. Other essential appliances such as water treatment plants and effluent treatment plants run six hours a day starting from 10.00 a.m. The washing machines and dryers run eight hours a day starting from 8.00 a.m. Apart from these main loads, some small loads such as ceiling fans and lights are ON for 24 h in different parts of the factory. During the weekend, the significant loads are the knitting machines, along with a few light and ceiling fan loads in use. The operation of knitting machines is supported through four 250 kVA uninterruptable power supply (UPS) units so that during any power interruption, the machines can operate continuously, until the problem is resolved within the shortest possible time.

The power system in the factory is modelled as an industrial MG that operates in off-grid mode. There is a provision to connect this industrial MG to the nearby centralized grid. The loads with their maximum power consumption are given in Table 3 and the single line diagram (SLD) is given in Figure 4. Most of the loads in this factory are induction motors resulting in large reactive power consumption. The total system loss found from simulation is 0.05 MW and 0.17 MVAR. The factory has three generators having a total capacity of three MVA to supply the loads during off-grid operation. The control modes of the generators are voltage-Q droop control. The description of the machines inside this facility has been collected by field inspection and then modelled following available dynamic models given in [48].

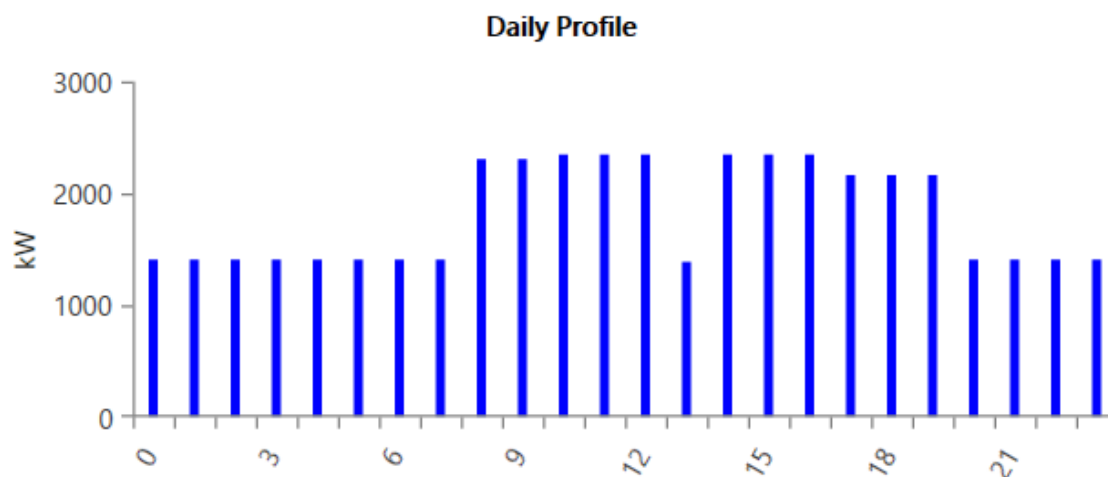


Figure 3. Daily load profile of the system.

Table 3. Loads in the RMG factory.

Serial No.	Machine Type	Maximum Power Per Unit (kW)	Number of Units	Bus Location
1	Auto knitting machine	1.28	656	DB-3F
2	Sewing machine	0.2	177	DB-1F, DB-2F
3	Manual linking machine	0.55	566	DB-1F, DB-2F
4	Iron table	0.7	98	DB-1F, DB-2F
5	Washing machine	4	6	DB-GF
6	Water treatment plant	1	5	DB-WTP
7	Effluent treatment plant	15	2	DB-ETP
8	Blower	75	1	DB-BOILER
9	Dryer 1	2.5	25	DB-DRYER
10	Dryer 2	5.2	12	DB-GF
11	Compressor 1	145	1	DB-CHILLER
12	Compressor 2	75	1	DB-CHILLER
13	Compressor 3	40	2	DB-DRYER
14	Panel machine	0.37	10	DB-GF
15	Fan coil unit 1	17	6	DB-3F
16	Fan coil unit 2	0.7	34	DB-GF, DB-1F, DB-3F, DB-4F
17	Fan coil unit 3	7	1	DB-2F
18	Exhaust fan 1	0.4	45	DB-DRYER, DB-GF, DB-1F, DB-2F, DB-3F
19	Exhaust fan 2	1.1	18	DB-GF, DB-1F, DB-2F
20	Celling fan	0.075	361	DB-GF, DB-1F, DB-2F
21	Air handling unit	5	2	DB-G.ROOM, DB-EMERGENCY
22	Cooling tower fan	4	5	DB-CHILLER
23	Lift	22	2	DB-4F
24	Pump 1	2.2	1	DB-4F
25	Pump 2	10	2	DB-PUMP
26	Pump 3	174	1	DB-FIRE PANEL
27	Pump 4	4	3	DB-PUMP
28	Cooling water pump	10	10	DB-CHILLER
29	Motor 1	2.2	1	DB-3F
30	Motor 2	1.1	3	DB-GF
31	Total composite load (lights and others)	370.36	–	–

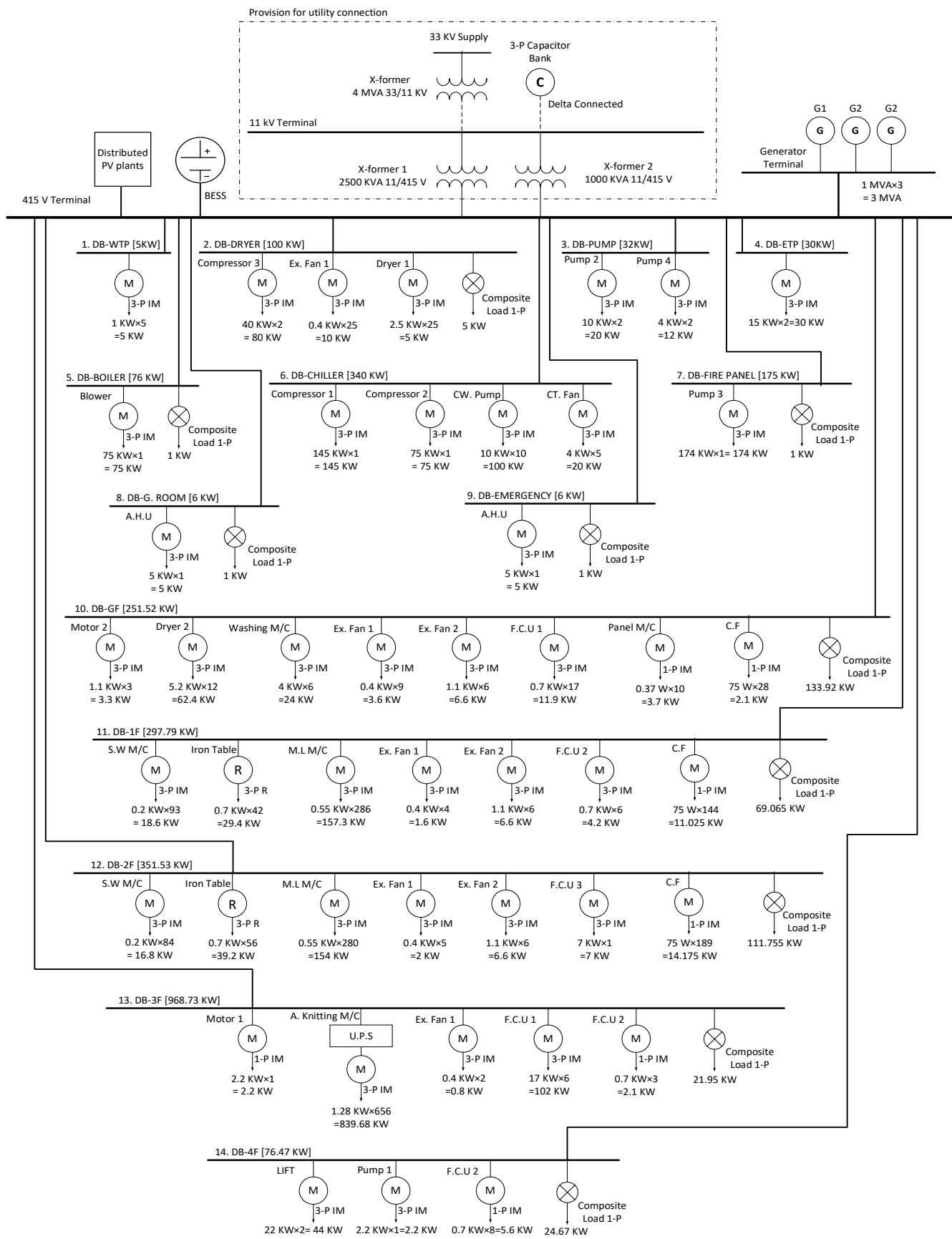


Figure 4. Power system single line diagram of the microgrid for RMG factory.

3.2. Simulation Results

To simulate the methodologies outlined in Section 2.2, tools used include DIgSILENT Power Factory 2020 for technical analysis and HOMER PRO for techno-economic analysis.

3.2.1. Step 1: Evaluate HC of Test System Considering Static Operational Issues and Find Its Robustness against Significant Disturbances

Once the system has been modelled in DIgSILENT Power Factory 2020 using data obtained from field inspection, the first step is to find the HC of different buses in the system. The bus that can host the maximum PV generation is identified as the location for future power injection from PV generators. The crucial criteria considered for calculating the HC are—the thermal limits, voltage limits, protection limits and short-circuit limits. The thermal limit was set for each component (lines, bus bars) to 100% loading. The voltage limit is set according to IEEE 1547-2018. The protection limit is set to take into account all necessary protection measures such as reverse power flow, relay tripping and total fault contribution (10% max). The short-circuit contribution limit was set by setting the fault clearing time to 0.2 s.

The busbar (bb) numbers, with their corresponding HC values, are presented in Table 4. Table 4 indicates that the 415 V bus has the maximum PV HC value of 5572 kW. Hence, PV generators can be planned to place at the 415 V terminal (see Figure 4).

Table 4. PV HC of different buses in the system.

Bus No	11 kV Terminal	415 V Terminal	bb1_WTP	bb2_DRYER	bb3_PUMP	bb4_ETP	bb5_BOILER	bb6_CHILLER
PV HC (kW)	2810	5572	200	527	224	222	261	1077
Bus No	bb7_Fire panel	bb8_G.room	bb9_Emergency	bb10_GF	bb11_1F	bb12_2F	bb13_3F	bb14_4F
PV HC (kW)	196	201	201	5508	4613	4053	3397	389

According to the HC analysis, the maximum PV HC value in the system under the static conditions given above is 5572 kW. However, the spatial area of the RMG factory for installing the distributed solar PV panels around the rooftops of the buildings and free space on the ground is limited. From the visual observations and considering the factor of 1000 kW capacity solar arrays may require around three hectares (i.e., 7.41 acres/30,000 square meters) of space, it is estimated that combined installation area in the specific RMG factory would accommodate about 2500 kW capacity of PV arrays. Therefore, the power system's area-constrained PV HC is set at 2500 kW, which is assigned as the target HC value. Now, to initiate further analysis, at the 415 V terminal, a PV system with a minimum size of 550 kW is deployed. In this step, the minimum size of the PV is taken as 550 kW as the off-grid MG is designed to have the solar PV output as much as possible, and with this, 550 kW of PV, along with the three generators, can meet the peak demand. To test the system dynamics, a time-domain RMS/EMT simulation has been executed for a time span of 20 s. In the simulation study, after the system is initialized at zero second, a disturbance (three phase fault) at the maximum load bus (bb14 3F) is initiated at five seconds, which is cleared at 5.2 s. In the presence of newly added PV, the system is deemed to be resilient if the post fault voltage and frequency remain within the IEEE std.1547-2018 allowed range.

After that, the size of the PV is steadily raised, with the post-fault voltage and frequency being measured each time. Figure 5 shows that when the PV capacity exceeds 1125 kW, the post-fault voltage and frequency exceed the permitted limits. As a consequence, the PV system is disconnected from the system since the PV controller is designed in such a manner that it can trip off the PV system in the event of a voltage or frequency threshold violation, according to IEEE standard. 1547-2018. As a result, the 1125 kW PV in this system can not sustain, and the rating of the PV system must be reduced. Lowering the

PV system to a rating of 1124 kW results in grid compatible post-fault voltage and frequency recovery, and hence can continue operation without tripping, as shown in Figure 6. As a result, the uncontrolled HC of this system may be determined as 1124 kW of PV, which keeps the system fault-resistant.

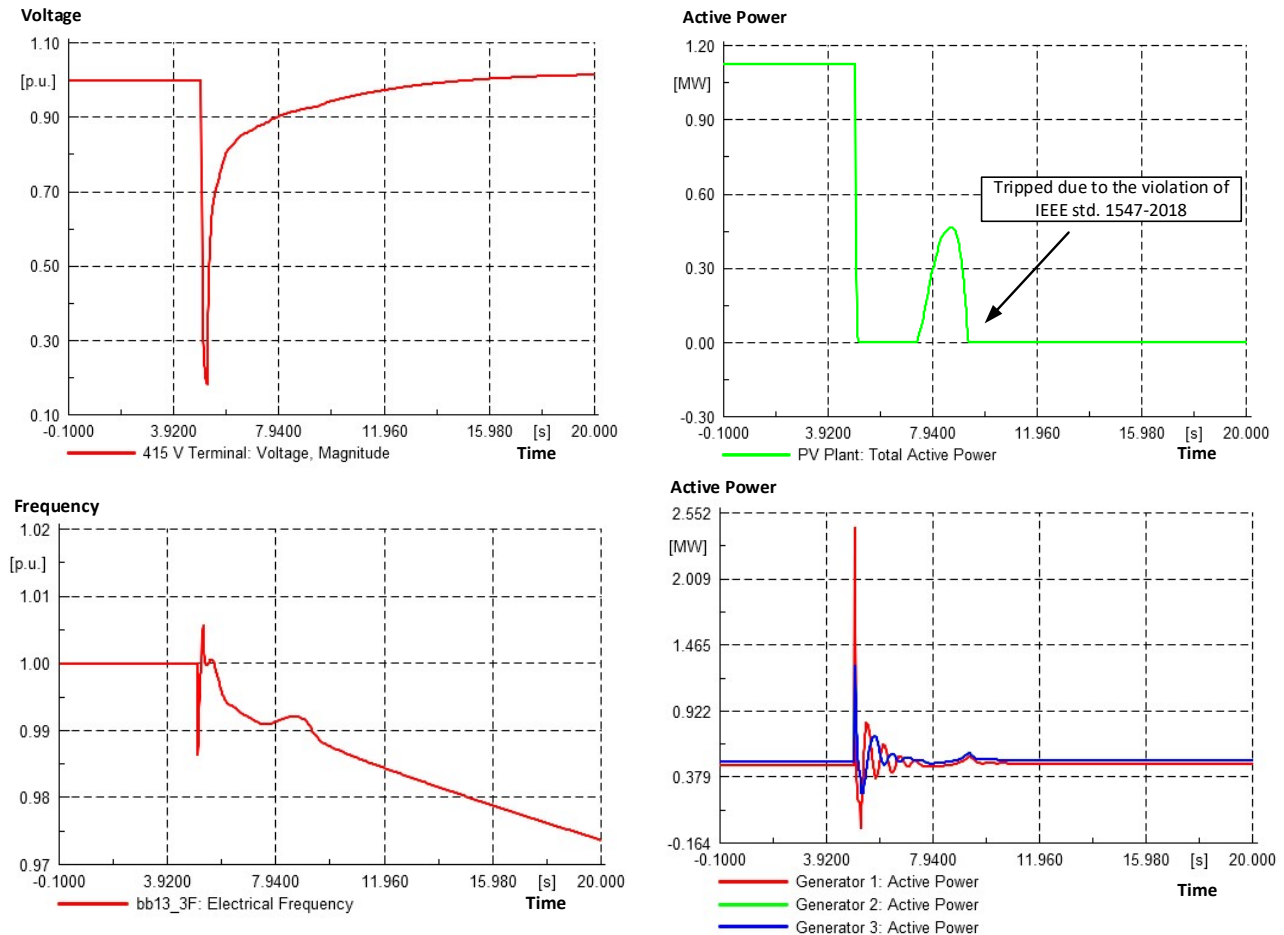


Figure 5. 415 V Terminal voltage (top left), system frequency (bottom left), PV Active power while PV size is at 1125 kW (top right) and active power of generators observed in step 1 (bottom right).

3.2.2. Step 2: Overcoming Technical Obstacles to Reach Target HC with BESS

To overcome the technical obstacles and reach the target HC of 2500 kW, a BESS is placed at the same bus of the PV system. As shown in Figure 7, 1125 kW of PV, which failed previously to support satisfactory operation, can sustain acceptable post-fault voltage and frequency by integrating 1.0 kVA of BESS. This indicates that placing a BESS can improve PV HC in terms of post-fault voltage and frequency. Now, PV and BESS size is increased step by step to reach the target PV HC.

When the PV size is gradually increased up to the target HC, i.e., 2500 kW, from Figure 8, it can be seen that the system can withstand the fault with 1237 kVA of BESS. Therefore, it can be said that the enhanced HC in the presence of 1237 kVA BESS is 2500 kW. More PV can be integrated with the increasing size of BESS if installation area expansion is possible in future. Zero shows the relationship between BESS size and managed HC of PV. From Figure 9, it is evident that the enhanced HC of PV increases with the increment of BESS size.

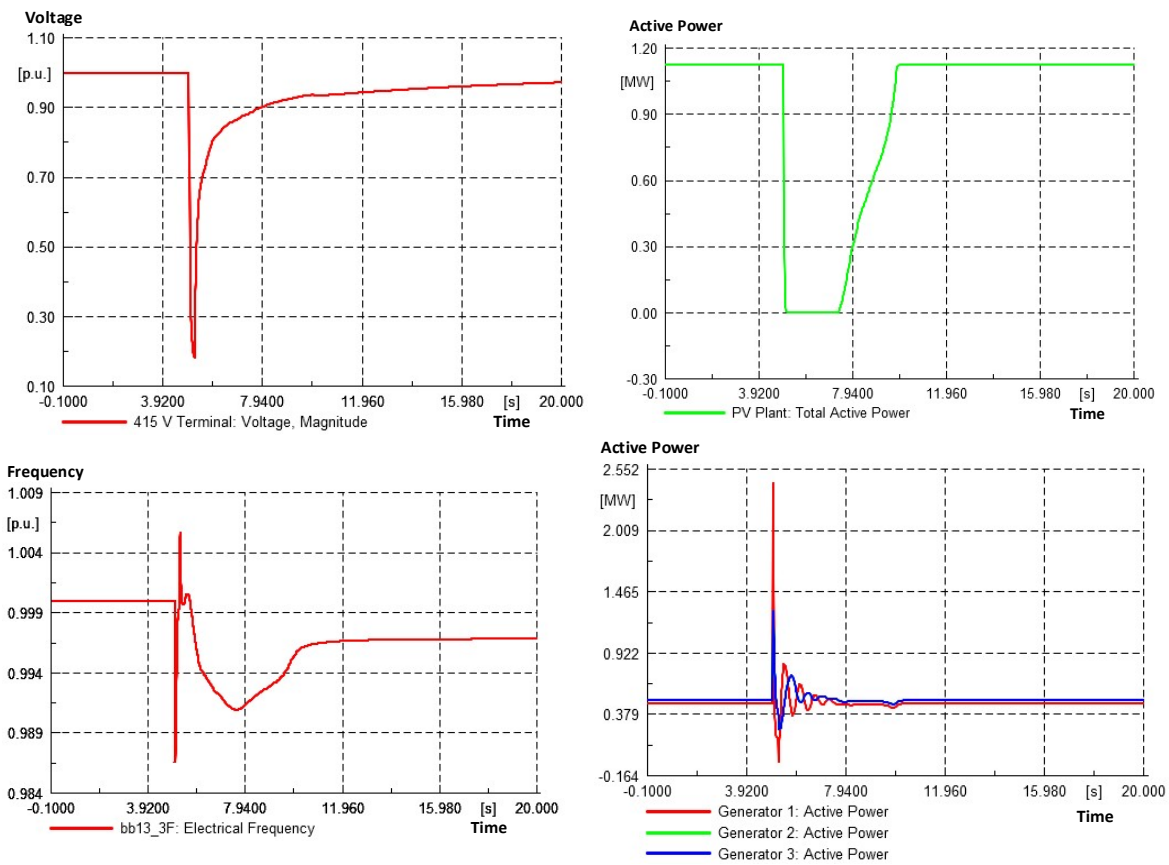


Figure 6. 415 V Terminal voltage (top left), system frequency (bottom left), PV Active power while PV size is 1124 kW (top right) and active power of generators observed in step 1 (bottom right).

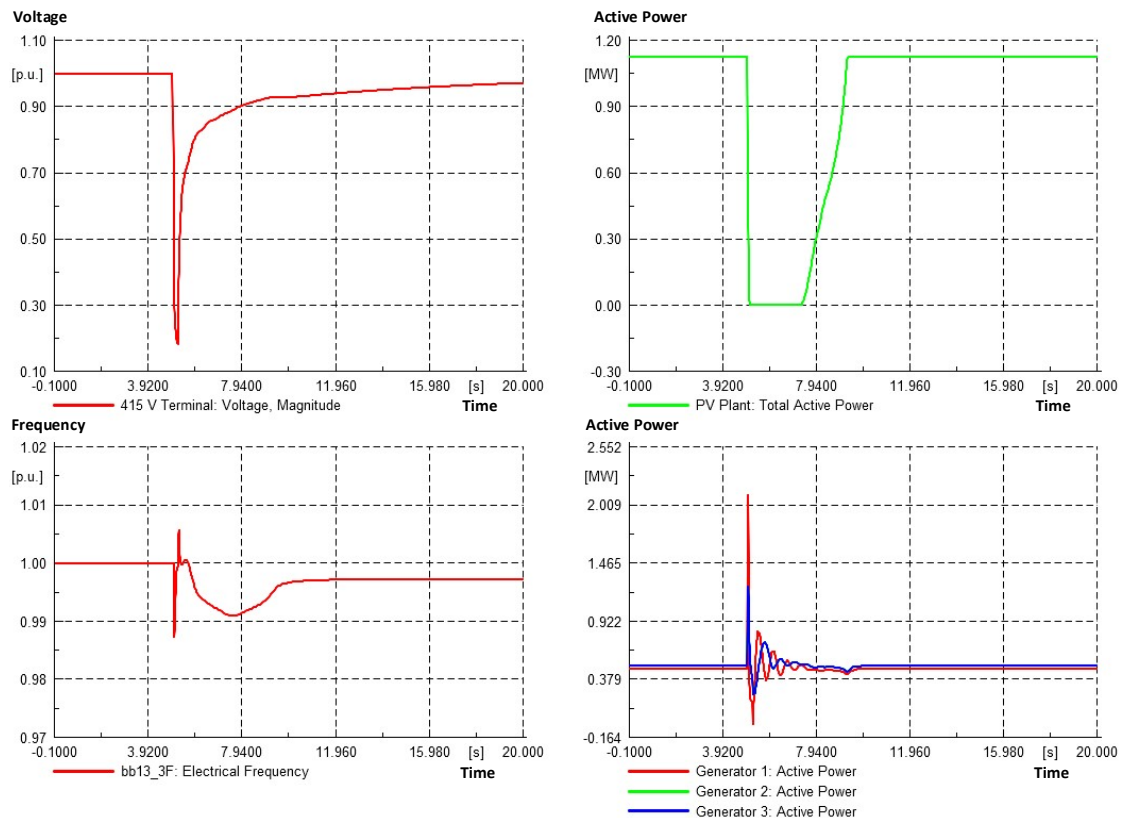


Figure 7. Cont.

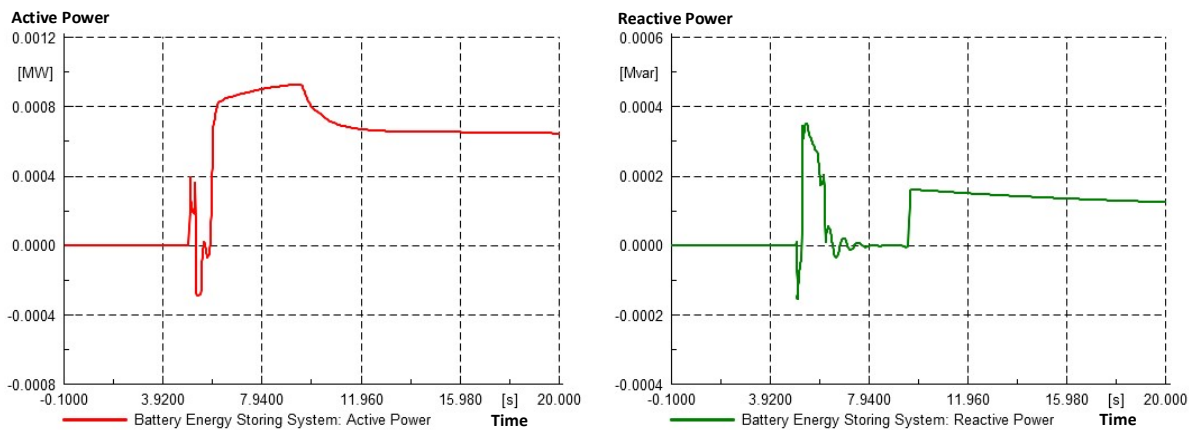


Figure 7. 415 V Terminal voltage (top left), PV Active power while the PV size is 1125 kW (top right), system frequency (mid left), Generator active power (mid right) and BESS active power (bottom left) and reactive power (bottom right) while the BESS size is 1.0 kVA in step 2.

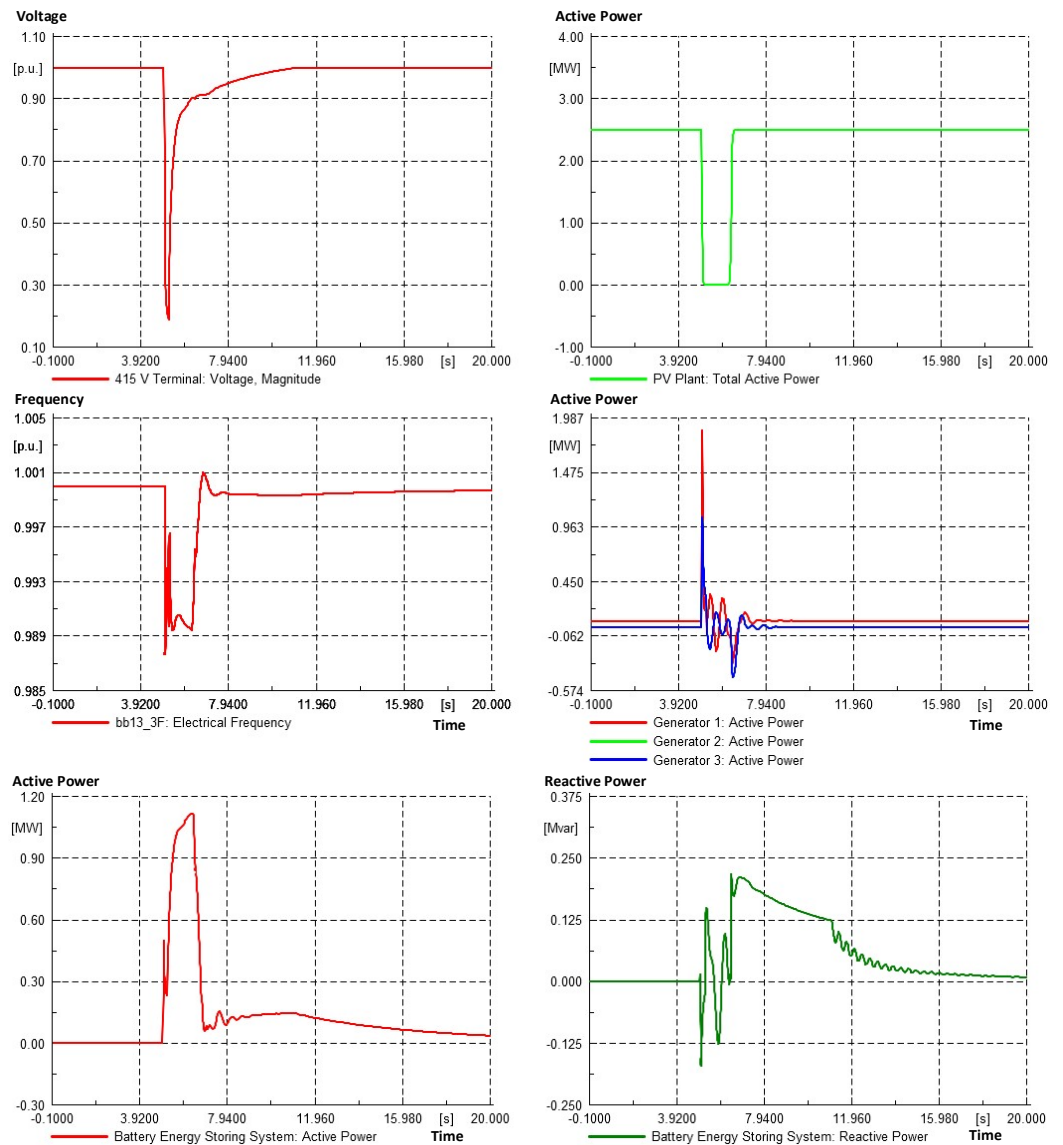


Figure 8. 415 V Terminal voltage (top left), PV Active power while the PV size is 2500 kW (top right), system frequency (mid left), Generator active power (mid right) and BESS active power (bottom left) and reactive power (bottom right) while the BESS size is 1237 kVA in step 2.

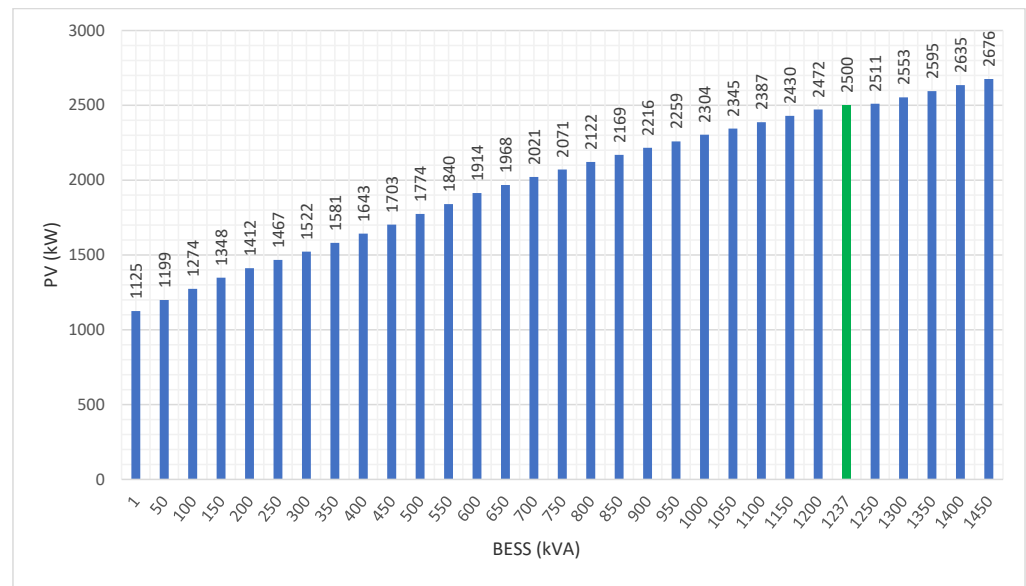


Figure 9. Enhanced HC with different sizes of BESS.

3.2.3. Economic Feasibility Study of HC Considering Techno-Economic Issues

HOMER Pro 3.14.4 is used to conduct the system optimization study and techno-economic analysis of the system. The schematic diagram of the energy system is presented in Figure 10. The drive of the techno-economic analysis is to realize if incorporating PV and BESS into the base system addressing the system technical constraints offers any financial benefits. Integrating renewables into either diesel-based or primarily grid-connected base power systems incurs a high initial cost. The energy storage system installation and maintenance costs also impact the levelized energy cost. However, integrating renewable energy resources incurs no fuel cost and a low operational and maintenance cost; and the life span of renewable energy systems is much longer. Taking these factors into account, a long-term computer-aided techno-economic analysis can indicate if installing PV-storage systems reduces the levelized cost of energy (LCOE). In this analysis, different system configurations are simulated during the optimization process to find the best system configuration satisfying the technical constraints at the lowest life-cycle cost. Recent cost information from the local market and relevant other information for the techno-economic analysis are provided in Table 5.

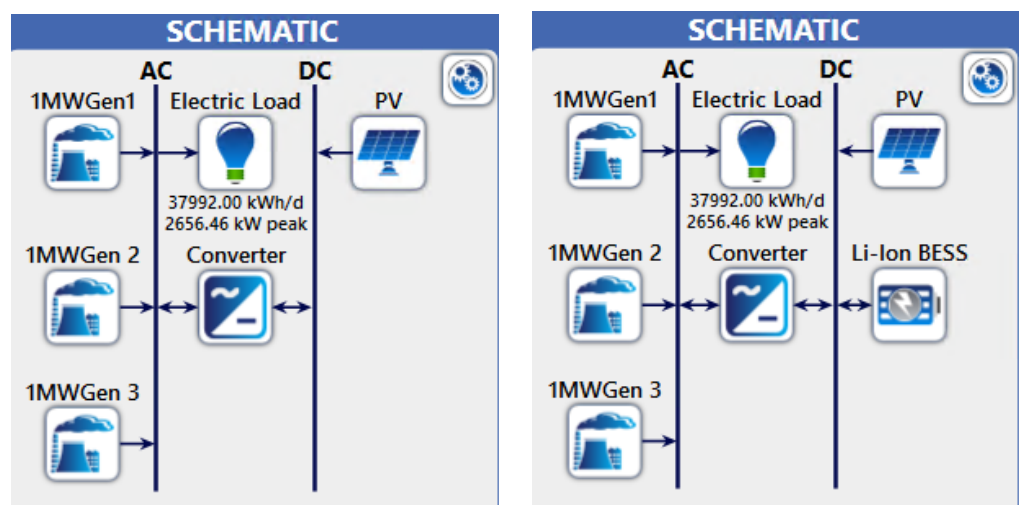


Figure 10. Schematic diagram of the energy system.

Table 5. Data for Techno-Economic Analysis.

Diesel Generator System Parameter		Solar PV System Parameter		Battery System Parameter	
System Parameter	Value/Information	System Parameter	Value/Information	System Parameter	Value/Information
Number of Operating Generators	03	Capital Cost (BDT */kWp)	50,000.00	Technology	Li-Ion Battery bank
Capacity of Identical Generators (kW)	1000	Replacement Cost (BDT/kWp)	50,000.00	Nominal Capacity (kWh/unit)	1.00
Minimum Loading Ratio (%)	25	Operation and Maintenance Cost (BDT/Year)	5000.00	Capital Cost (BDT/unit)	3500.00
Minimum Run Time (Minute)	30	Lifetime (Years)	25.00	Replacement Cost (BDT/unit)	3500.00
Capital Cost (BDT/kW)	300,000.00	Derating Factor (%)	90.00	Operation and Maintenance Cost (BDT/Year)	0.00
Replacement Cost (BDT/kW)	300,000.00	Inverter (bi-directional and grid-tied)		Minimum State of Charge (%)	20.00
Operation and Maintenance Cost (BDT/hour)	10.000	Capital Cost (BDT/kW)	45,000.00	Minimum storage life (Years)	2.00
Lifetime Running hours	15,000.00	Replacement Cost (BDT/kW)	45,000.00		
Diesel Price (BDT/Litre)	65	Operation and Maintenance Cost (BDT/Year)	0.0		
		Efficiency (%)	98.00		
		Lifetime (Years)	15.00		
		Project Information			
Expected Inflation Rate (%)	6.70	Expected Nominal Discount Rate (%)	7.00	Project Lifetime (Years)	20.00

* Conversion rate: 1 BDT = 0.012 USD.

Enhanced BESS size allows the system to incorporate an enhanced PV generation while maintaining system robustness (as seen in step 2). The LCOE with different BESS sizes and corresponding maximum PV sizes are brought together and plotted in Figure 11 to understand better the economic scenarios where each scenario is fault-tolerant. Without the support from BESS, the power system not only faces resiliency (fault tolerance) issues but also has the highest LCOE for all the entries in the long term simulation. It appears that when the BESS size is increased, the LCOE should shoot as well. However, the study outcome has demonstrated in Figure 11 that increasing BESS size reduces the LCOE primarily due to the enhancement in the hosting capacity of PV in the system.

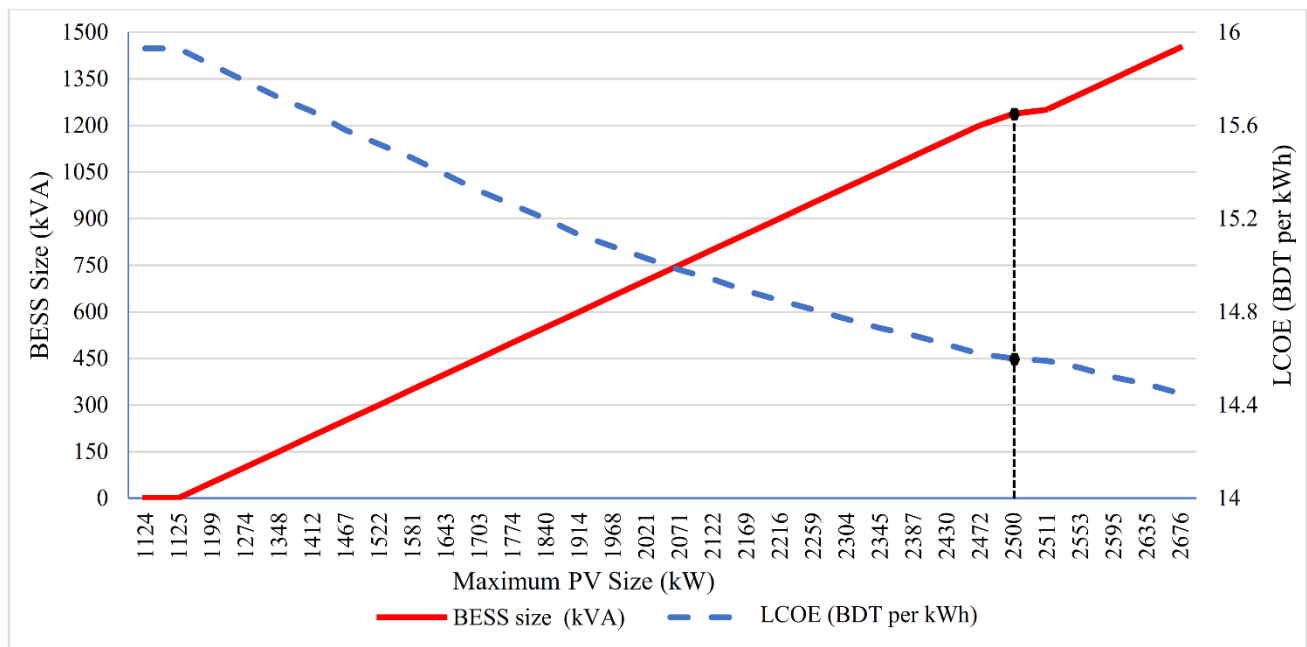


Figure 11. LCOE for different PV sizes with different BESS sizes.

Even if the change in LCOE from one situation to the next is not substantial, different configuration sets have different operating costs. From Figure 11, it can be observed that the highest LCOE (BDT 15.93/kWh) is reached with 1124 kW PV and no BESS. On the other hand, the lowest COE (BDT 14.60/kWh) is achieved with 2500 kW PV and 1237 kVA

BESS in the conceivable scenario. Another potential scenario exists where the LCOE is BDT 15.03/kWh for having 2021 kW of PV and 700 kVA of BESS. Table 6 provides a comparison of these three possibilities. In contrast to the highest LCOE scenario, the yearly operating cost is lowered by BDT 18 million, equal to around USD 212,000 (1 BDT = 0.012 USD) per year in the lowest LCOE scenario. The resultant LCOE found in the study offers a promising outcome as another study conducted in 2021 by Islam et al., for an off-grid community in Bangladesh revealed that the LCOE for the 331 kW annual peak demand is BDT 21.39 per kW for a hybrid diesel-PV-Hydrogen-battery-based microgrid [38].

Table 6. Comparison between scenarios with lowest and highest COEs.

PV (kW)	BESS (kVA)	LCOE (BDT/kWh)	LCOE (USD/kWh)	Operating Cost (Million BDT/yr)	Operating Cost (Million USD/yr)	Renewable Fraction (%)	Total Fuel (L/yr)	PV Production (kWh/yr)
1124	0	15.93	0.1875	216	2.54	11.8	3,228,698	1,693,984
2021	700	15.03	0.1769	200	2.35	20.6	2,910,531	3,045,856
2500	1237	14.60	0.1719	192	2.26	24.8	2,759,028	3,767,759

Figures 12 and 13 present the results of the optimization surface plot. These illustrations present a concrete relation among PV capacity, battery capacity, fuel usage, CO₂ emission and the renewable share in the system design. It can be observed that the diesel usage abruptly drops when the system is integrated with more than 1000 kW capacity of the PV system. Up to 1000 kW of PV capacity, diesel has been the primary source of supply as PV capacity was small. Due to the PV output variability, operating reserve limits and the diesel engine's technical constraints (minimum run time and minimum loading), diesel generators had to be kept ON for the maximum time. Consequently, fuel consumption did not decrease much. When more and more PV got installed beyond 1000 kW, the engine technical issues did not hit the barrier limits due to more PV output in the system. Thus, the system dynamics and dispatch algorithm allowed the PV to overtake the diesel generators as the primary supply source during the sunshine hours. So, the more the PV and battery capacity are integrated, the more the amount of diesel consumption dropped and consequentially, the COE improved. These situations can be observed in Figure 12. In this figure, a different color denotes a different amount of diesel consumption in liters.

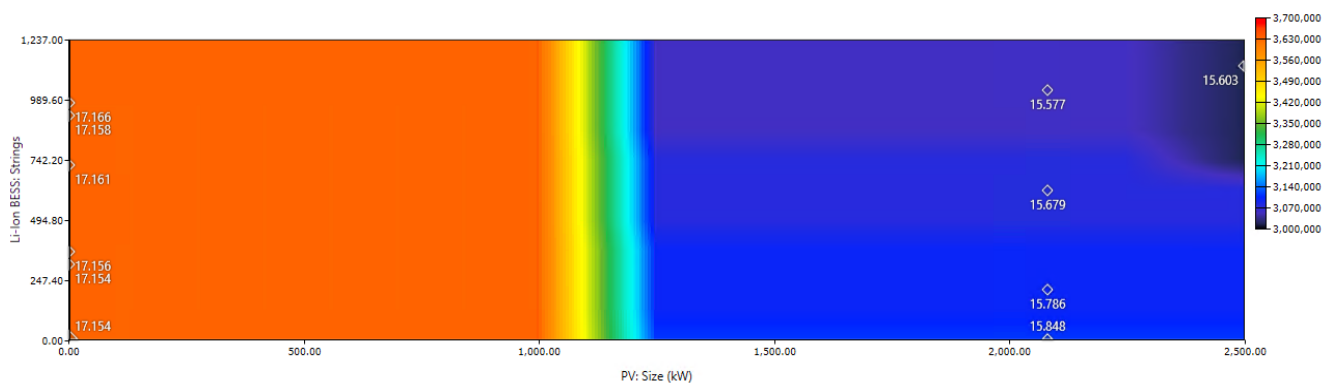


Figure 12. Optimization surface plot with total fuel and COE superimposed.

Similarly, when more PV and battery capacity are integrated, the amount of CO₂ emission decreases. Along with Figure 12, from Figure 13, we can also observe that when the PV capacity goes above 1000 kW, the emission of CO₂ starts decreasing abruptly. As the renewable fraction/share (PV hosting capacity) increased, significant emissions decreased as diesel consumption decreased. These two figures validate the basic understanding of the research conducted.

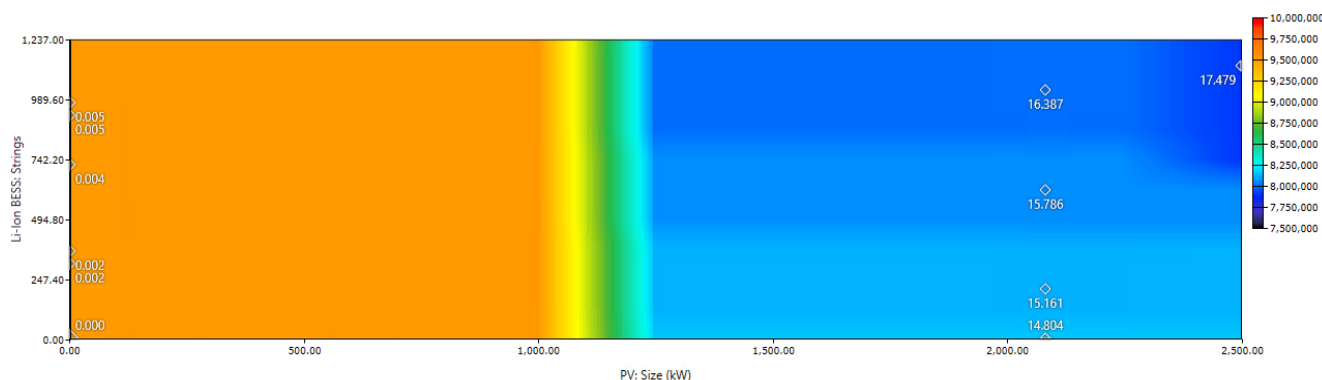


Figure 13. Optimization surface plot with CO₂ emission and renewable fraction superimposed.

A comparison is given in Table 7 for a better understanding of the contribution of this work with other similar techno-economic analyses presented in the literature. Other than the references [20–25], most of the sites of the studies chosen are identical to the present study, i.e., are in the off-grid areas. It can also be seen that none of the studies have checked the system robustness, i.e., fault tolerance as a limiting factor for the PV hosting capacity determination. Some studies given in Table 7 show lower LCOE than the COE obtained in this study as the optimization algorithm used in those studies addressed different objective functions and more relaxed system constraints, such as flexible PV and BESS sizing. The straightforward comparison of the LCOEs obtained in different studies can not be considered as the decisive parameter for judging the design excellence of systems. As the economic parameters of any system are very much case and location-specific, it would be unwise to compare the LCOEs of different systems for different countries having a different market structures. Hence, based on the authors’ expertise of the local market and socio-economic condition, it can be stated that the LCOE obtained in this study is a reasonable one for the intended customer, which is remote industries.

Table 7. Comparison between this work with other similar studies.

Reference No	Grid Connectivity	Energy System	HC Analysis	System Robustness Check	Optimization	Lowest Levelized Cost of Energy (LCOE)
[14]	Off-grid	Diesel, PV + Diesel, PV + Diesel + Battery, Wind + Diesel, Wind + Diesel + Battery, Diesel + Battery, PV + Wind + Diesel, PV + Wind + Diesel + Battery	No	No	Yes	0.246 USD/kWh
[15]	Off-grid	PV + Wind + Diesel + Battery, PV + Battery, Wind + Diesel + Battery, Diesel	No	No	Yes	0.29 USD/kWh
[16]	Off-grid	PV, PV + Battery	No	No	No	0.15 USD/kWh
[17]	Off-grid	PV	No	No	No	0.045 USD/kWh
[18]	Off-grid	PV, Wind, PV + Wind	No	No	Yes	–
[19]	Off-grid	PV	No	No	Yes	–
[20]	On-grid and off-grid	Grid + PV, PV + Battery	No	No	Yes	0.060 USD/kWh
[21]	On-grid and off-grid	Grid + PV, Grid + PV + Battery, PV + Battery	No	No	Yes	0.0581 USD/kWh
[22]	On-grid	PV	No	No	Yes	0.031 USD/kWh
[23]	On-grid	Grid + PV + Wind + Battery	Yes	No	Yes	–
[24]	On-grid	Grid + PV	Yes	No	No	–
[25]	On-grid	Grid + PV, Grid + Wind, Grid + PV + Wind	No	No	Yes	0.0702 USD/kWh
This paper	Off-grid	Diesel + PV + Battery	Yes	Yes	Yes	0.1719 USD/kWh

4. Conclusions

Solar PV systems are rising day by day, particularly in industrial microgrids, as a result of their cost-effectiveness and environmental friendliness. As part of the commitment to carbon-free emissions, various industries worldwide are ramping up their use of green energy. PV hosting capacity evaluation is thus required for better integration and performance of solar PV systems before integrating them into a power system. A conventional theoretical hosting capacity mechanism cannot meet the necessity to provide

system resilience against any disruption. Hence, this study proposed a unique method and attempted in computing both the controlled and uncontrolled hosting capacity of PV systems by introducing system disturbance in the means of electrical faults (three-phase short circuits). A system techno-economic analysis has also been conducted along with the technical study. The research realized that incorporating battery energy storage systems (BESS) into the microgrid enhanced PV hosting capacity for the system. These unique PV generation enhancement and systematic strategy studies have been applied for the industrial electrical network in a ready-made garment (RMG) factory in Bangladesh, having a distinctive demand pattern and space constraints to uptake a high PV generation facility.

The unique study conducted a detailed technical and long-term techno-economic analysis and found that extending the size of the battery energy storage system not only enhanced the PV hosting capacity in the industrial microgrid but also reduced the leveled cost of energy. According to the study's findings, integrating 2500 kW of PV along with a 1237 kVA battery bank incurs an energy cost of nearly USD 0.1719 per kWh for an off-grid Bangladeshi RMG factory having a daily peak load of 2656.46 kW. Considering the local socio-economic and geographical context and constraints, the revealed energy cost offers a promising outcome.

The study has been able to successfully demonstrate that by taking the suitable amount of PV-BESS systems to offset diesel consumption in a less reliable grid-connected system, the industrial establishments, like RMG factories, would not only benefit from the environmental and social advantages offered by the renewable energy-based systems but also make a financial profit. This would not only help the RMG factories individually but would also assist any country like Bangladesh in promoting the green RMG factories to the world to attract more investment and, side-by-side, address one of the UN SDG goals such as SDG7. Future studies would focus on analyzing system dynamics with more complicated technical issues, which may disrupt system resiliency in the presence of high PV penetration in an industrial microgrid operating in off-grid mode. The economic viability of any improvement approach for preserving system resilience while boosting the PV share will also be examined in future research.

Author Contributions: Conceptualization, S.A., A.E.R., T.J. and T.A. (Tareq Aziz); methodology, A.E.R., T.J. and T.A. (Tareq Aziz); software, S.A. and A.E.R.; validation, S.A., A.E.R., T.J. and T.A. (Tareq Aziz); formal analysis, S.A., A.E.R., T.J. and T.A. (Tareq Aziz); investigation, S.A., A.E.R., T.J. and T.A. (Tareq Aziz); resources, S.A. and S.U.A.; data curation, S.U.A.; writing—original draft preparation, A.E.R. and T.J.; writing—review and editing, S.A., A.E.R., M.S.H.L., T.J., T.A. (Tareq Aziz), M.R.S., A.R., T.A. (Talal Alharbi) and M.M.H.; visualization, S.A., A.E.R. and T.J.; supervision, T.A. (Tareq Aziz); project administration, M.S.H.L., T.J., T.A. (Tareq Aziz), M.R.S., A.R., T.A. (Talal Alharbi) and M.M.H.; funding acquisition, M.S.H.L., T.J., M.R.S., A.R., T.A. (Talal Alharbi) and M.M.H. All authors have read and agreed to the published version of the manuscript.

Funding: The researchers would like to thank the Deanship of Scientific Research, Qassim University, Saudi Arabia for funding the publication of this project.

Institutional Review Board Statement: Not applicable.

Informed Consent Statement: Not applicable.

Data Availability Statement: Not applicable.

Acknowledgments: The researchers would like to thank the Deanship of Scientific Research, Qassim University, Saudi Arabia for funding the publication of this project.

Conflicts of Interest: The authors declare no conflict of interest.

Abbreviations

Summary of the notations and symbols.

Notations/Symbols	Meaning
SDG	Sustainable development goals
RMG	Ready-made garment
PV	Photovoltaics
HC	Hosting capacity
MG	Microgrid
BESS	Battery energy storage system
LCOE	Levelized cost of energy
IES	Illuminating engineering society
THD	Third harmonic distortion
DG	Distributed generation
DB	Distribution board
bb	Busbar

References

1. Tabassum, M. Top 10 Garments Exporting Countries of the World in 2020 | Top Textiles Exporting Countries. Textfiles BD, 28 November 2021. Available online: <https://www.textfilesbd.com/factories/top-10-garments-exporting-countries-of-the-world-in-2021/> (accessed on 22 May 2022).
2. Desk Report. Bangladesh Has Highest Number of LEED Platinum-Rated Garment Factories. *TextileToday*, 19 September 2021. Available online: <https://www.textiletoday.com.bd/bangladesh-highest-number-leed-platinum-rated-garment-factories/> (accessed on 22 May 2022).
3. Islam, S. Bangladeshi apparel makers opt for rooftop solar. *PV Magazine*, 4 January 2021. Available online: <https://www.pv-magazine.com/2021/01/04/bangladeshi-apparel-makers-opt-for-rooftop-solar/> (accessed on 22 May 2022).
4. Jamal, T.; Urme, T.; Shafiullah, G.M.; Shahnia, F. Using Experts' Opinions and Multi-Criteria Decision Analysis to Determine the Weighing of Criteria Employed in Planning Remote Area Microgrids. In Proceedings of the 2018 International Conference and Utility Exhibition on Green Energy for Sustainable Development (ICUE), Phuket, Thailand, 24–26 October 2018; pp. 1–7. [CrossRef]
5. Jamal, T.; Urme, T.; Shafiullah, G.M. Planning of Off-Grid Power Supply Systems in Remote Areas Using Multi-Criteria Decision Analysis. *Energy* **2020**, *201*, 117580. [CrossRef]
6. El-houari, H.; Allouhi, A.; Salameh, T.; Kousksou, T.; Jamil, A.; El Amrani, B. Energy, Economic, Environment (3E) Analysis of WT-PV-Battery Autonomous Hybrid Power Plants in Climatically Varying Regions. *Sustain. Energy Technol. Assess.* **2021**, *43*, 100961. [CrossRef]
7. Vella, H. Microgrids—The Key to Providing Electricity in Rural Communities? Available online: <https://www.power-technology.com/features/featuremicrogrids-the-key-to-providing-electricity-to-the-energy-poor-4314517/> (accessed on 13 July 2021).
8. Ali, L.; Shahnia, F. Impact of Annual Load Growth on Selecting the Suitable Sustainable Standalone System for an Off-Grid Town in Western Australia. In Proceedings of the 2016 IEEE International Conference on Power System Technology POWERCON 2016, Wollongong, NSW, Australia, 28 September–1 October 2016; pp. 2–6. [CrossRef]
9. Jamal, T.; Shoeb, M.A.; Shafiullah, G.M.; Carter, C.E.; Urme, T. A Design Consideration for Solar PV-Diesel Remote Electricity Network: Australia Perspective. In Proceedings of the IEEE PES Innovative Smart Grid Technologies Conference Europe, Ljubljana, Slovenia, 9–12 October 2016; IEEE Computer Society: Washington, DC, USA, 2016; pp. 821–826.
10. Ismael, S.M.; Abdel Aleem, S.H.E.; Abdelaziz, A.Y.; Zobaa, A.F. State-of-the-Art of Hosting Capacity in Modern Power Systems with Distributed Generation. *Renew. Energy* **2019**, *130*, 1002–1020. [CrossRef]
11. Power and Water Corporation. *Solar/Diesel Mini-Grid Handbook*; Australian Government, Australian Renewable Energy Agency: Canberra City, ACT, Australia, 2019.
12. Jamal, T.; Urme, T.; Calais, M.; Shafiullah, G.M.; Carter, C. Technical Challenges of PV Deployment into Remote Australian Electricity Networks: A Review. *Renew. Sustain. Energy Rev.* **2017**, *77*, 1309–1325. [CrossRef]
13. Hosseini, Z.S.; Khodaei, A. Dynamic Solar Hosting Capacity Calculations in Microgrids. In Proceedings of the CIGRE US National Committee 2018 Grid of the Future Symposium, Schipol, The Netherlands, 28–31 October 2018.
14. Salehin, S.; Rahman, M.M.; Islam, A.K.M.S. Techno-Economic Feasibility Study of a Solar PV-Diesel System for Applications in Northern Part of Bangladesh. *Int. J. Renew. Energy Res.* **2015**, *5*, 1220–1229. [CrossRef]
15. Das, B.K.; Alotaibi, M.A.; Das, P.; Islam, M.S.; Das, S.K.; Hossain, M.A. Feasibility and Techno-Economic Analysis of Stand-Alone and Grid-Connected PV/Wind/Diesel/Batt Hybrid Energy System: A Case Study. *Energy Strateg. Rev.* **2021**, *37*, 100673. [CrossRef]
16. Chandel, M.; Agrawal, G.D.; Mathur, S.; Mathur, A. Techno-Economic Analysis of Solar Photovoltaic Power Plant for Garment Zone of Jaipur City. *Case Stud. Therm. Eng.* **2014**, *2*, 1–7. [CrossRef]

17. Shah, S.A.A.; Das Valasai, G.; Memon, A.A.; Laghari, A.N.; Jalbani, N.B.; Strait, J.L. Techno-Economic Analysis of Solar PV Electricity Supply to Rural Areas of Balochistan, Pakistan. *Energies* **2018**, *11*, 1777. [[CrossRef](#)]
18. Al-Ghussain, L.; Samu, R.; Taylan, O.; Fahrioglu, M. Techno-Economic Comparative Analysis of Renewable Energy Systems: Case Study in Zimbabwe. *Inventions* **2020**, *5*, 27. [[CrossRef](#)]
19. Bhagavathy, S.M.; Pillai, G. PV Microgrid Design for Rural Electrification. *Designs* **2018**, *2*, 33. [[CrossRef](#)]
20. Poudyal, R.; Loskot, P.; Parajuli, R. Techno-Economic Feasibility Analysis of a 3-KW PV System Installation in Nepal. *Renew. Wind. Water Sol.* **2021**, *8*, 5. [[CrossRef](#)]
21. Mekonnen, T.; Bhandari, R.; Ramayya, V. Modeling, Analysis and Optimization of Grid-integrated and Islanded Solar Pv Systems for the Ethiopian Residential Sector: Considering an Emerging Utility Tariff Plan for 2021 and Beyond. *Energies* **2021**, *14*, 3360. [[CrossRef](#)]
22. Husain, A.A.F.; Phesal, M.H.A.; Ab Kadir, M.Z.A.; Ungku Amirulddin, U.A. Techno-Economic Analysis of Commercial Size Grid-Connected Rooftop Solar Pv Systems in Malaysia under the Nem 3.0 Scheme. *Appl. Sci.* **2021**, *11*, 10118. [[CrossRef](#)]
23. Rawa, M.; Abusorrah, A.; Al-Turki, Y.; Mekhilef, S.; Mostafa, M.H.; Ali, Z.M.; Aleem, S.H.E.A. Optimal Allocation and Economic Analysis of Battery Energy Storage Systems: Self-Consumption Rate and Hosting Capacity Enhancement for Microgrids with High Renewable Penetration. *Sustainability* **2020**, *12*, 10144. [[CrossRef](#)]
24. Arshad, A.; Lindner, M.; Lehtonen, M. An Analysis of Photo-Voltaic Hosting Capacity in Finnish Low Voltage Distribution Networks. *Energies* **2017**, *10*, 1702. [[CrossRef](#)]
25. Tazay, A. Techno-Economic Feasibility Analysis of a Hybrid Renewable Energy Supply Options for University Buildings in Saudi Arabia. *Open Eng.* **2020**, *11*, 39–55. [[CrossRef](#)]
26. Fachrizal, R.; Ramadhani, U.H.; Munkhammar, J.; Widén, J. Combined PV–EV Hosting Capacity Assessment for a Residential LV Distribution Grid with Smart EV Charging and PV Curtailment. *Sustain. Energy Grids Netw.* **2021**, *26*, 100445. [[CrossRef](#)]
27. Christiaanse, T.V.; Loonen, R.C.G.M.; Evins, R. Techno-Economic Optimization for Grid-Friendly Rooftop PV Systems—A Case Study of Commercial Buildings in British Columbia. *Sustain. Energy Technol. Assess.* **2021**, *47*, 101320. [[CrossRef](#)]
28. Sanwar Hossain, M.; Islam, K.Z.; Alharbi, A.G.; Shafiullah, M.; Islam, M.R.; Fekih, A. Optimal Design of a Hybrid Solar PV/BG-Powered Heterogeneous Network. *Sustainability* **2022**, *14*, 2201. [[CrossRef](#)]
29. Badal, F.R.; Das, P.; Sarker, S.K.; Das, S.K. A Survey on Control Issues in Renewable Energy Integration and Microgrid. *Prot. Control. Mod. Power Syst.* **2019**, *4*, 8. [[CrossRef](#)]
30. Ding, K.; Li, W.; Qian, Y.; Hu, P.; Huang, Z. Application of User Side Energy Storage System for Power Quality Enhancement of Premium Power Park. *Sustainability* **2022**, *14*, 3668. [[CrossRef](#)]
31. Mukhopadhyay, B.; Das, D. Optimal Multi-Objective Long-Term Sizing of Distributed Energy Resources and Hourly Power Scheduling in a Grid-Tied Microgrid. *Sustain. Energy Grids Netw.* **2022**, *30*, 100632. [[CrossRef](#)]
32. Zhou, J.; Tsiannikas, S.; Birnie, D.P.; Coit, D.W. Economic and Resilience Benefit Analysis of Incorporating Battery Storage to Photovoltaic Array Generation. *Renew. Energy* **2019**, *135*, 652–662. [[CrossRef](#)]
33. Tumiran; Nafis, A.S.T.; Sarjiya; Putranto, L.M.; Indrawan, H. Determination of PV Hosting Capacity in Rural Distribution Network: A Study Case for Bantul Area. *Int. J. Renew. Energy Res.* **2019**, *9*, 1116–1124.
34. Arif, S.; Rabbi, A.E.; Jamal, T.; Aziz, T. Behavioural Study of a Remote Power System with High PV Penetration during a State of Emergency. In Proceedings of the 2020 International Conference on Smart Grids and Energy Systems (SGES), Perth, Australia, 23–26 November 2020; Institute of Electrical and Electronics Engineers Inc.: Piscataway, NJ, USA, 2020; pp. 590–595.
35. Bajaj, M.; Kumar Singh, A. Hosting Capacity Enhancement of Renewable-Based Distributed Generation in Harmonically Polluted Distribution Systems Using Passive Harmonic Filtering. *Sustain. Energy Technol. Assess.* **2021**, *44*, 101030. [[CrossRef](#)]
36. Liu, D.; Wang, C.; Tang, F.; Zhou, Y. Probabilistic Assessment of Hybridwind-Pv Hosting Capacity in Distribution Systems. *Sustainability* **2020**, *12*, 2183. [[CrossRef](#)]
37. Fatima, S.; Püvi, V.; Lehtonen, M. Review on the PV Hosting Capacity in Distribution Networks. *Energies* **2020**, *13*, 4756. [[CrossRef](#)]
38. Mohammadi, P.; Mehraeen, S. Challenges of PV Integration in Low-Voltage Secondary Networks. *IEEE Trans. Power Deliv.* **2017**, *32*, 525–535. [[CrossRef](#)]
39. Iqbal, A.; Ayoub, A.; Waqar, A.; Ul-Haq, A.; Zahid, M.; Haider, S. Voltage Stability Enhancement in Grid-Connected Microgrid Using Enhanced Dynamic Voltage Restorer (EDVR). *AIMS Energy* **2021**, *9*, 150–177. [[CrossRef](#)]
40. Essackjee, I.A.; Ah King, R.T.F. Maximum Rooftop Photovoltaic Hosting Capacity with Harmonics as Limiting Factor—Case Study for Mauritius. In Proceedings of the 2019 International Conference on Advances in Big Data, Computing and Data Communication Systems (icABCD), Winterton, South Africa, 5–6 August 2019; Institute of Electrical and Electronics Engineers Inc.: Winterton, South Africa, 2019; pp. 1–6.
41. Akinyele, D.; Belikov, J.; Levron, Y. Challenges of Microgrids in Remote Communities: A STEEP Model Application. *Energies* **2018**, *11*, 432. [[CrossRef](#)]
42. Cetinkaya, H.B.; Kucuk, S.; Unaldi, M.; Gokce, G.B. A Case Study of a Successful Industrial Microgrid Operation. In Proceedings of the 2017 4th International Conference on Electrical and Electronic Engineering (ICEEE), Ankara, Turkey, 8–10 August 2017; pp. 95–98.
43. Haesen, E.; Minne, F.; Driesen, J.; Bollen, M. Hosting Capacity for Motor Starting in Weak Grids. In Proceedings of the 2005 International Conference on Future Power Systems, Amsterdam, The Netherlands, 16–18 November 2005; Volume 6. [[CrossRef](#)]

44. Aziz, T.; Al Masood, N.; Deeba, S.R.; Tushar, W.; Yuen, C. A Methodology to Prevent Cascading Contingencies Using BESS in a Renewable Integrated Microgrid. *Int. J. Electr. Power Energy Syst.* **2019**, *110*, 737–746. [[CrossRef](#)]
45. DIgSILENT GmbH. *PowerFactory 2020 SP3 User Manual*; DIgSILENT GmbH: Gomaringen, Germany, 2020.
46. *IEEE Std. 1547-2018*; IEEE Standard for Interconnection and Interoperability of Distributed Energy Resources with Associated Electric Power Systems Interfaces. Institute of Electrical and Electronics Engineers (IEEE): Piscataway, NJ, USA, 2018; ISBN 9781504446396.
47. HOMER Pro 3.14. Available online: <https://www.homerenergy.com/products/pro/docs/latest/index.html> (accessed on 18 August 2021).
48. Kundur, P.; Balu, N.J.; Lauby, M.G. *Power System Stability and Control*; McGraw-Hill: New York, NY, USA, 1994; ISBN 0070635153.